

# Nucleosomal histone protein protects DNA from iron-mediated damage

Helen U.Enright, Wesley J.Miller and Robert P.Hebbel\*

Division of Hematology, Department of Medicine, Box 480, University of Minnesota Medical School, Harvard Street at East River Road, Minneapolis, MN 55455, USA

Received April 16, 1992; Revised and Accepted June 11, 1992

## ABSTRACT

**Iron promotes DNA damage by catalyzing hydroxyl radical formation. We examined the effect of chromatin structure on DNA susceptibility to oxidant damage. Oxygen radicals generated by H<sub>2</sub>O<sub>2</sub>, ascorbate and iron-ADP (1:2 ratio of Fe<sup>2+</sup>:ADP) extensively and randomly fragmented protein-free DNA, with double-strand breaks demonstrable even at 1 μM iron. In contrast, polynucleosomes from chicken erythrocytes were converted to nucleosome-sized fragments by iron-ADP even up to 250 μM iron. Cleavage occurred only in bare areas where DNA is unassociated with histone. In confirmation, reassembly of nucleosomes from calf thymus DNA and chicken erythrocyte histone also yielded nucleosomes resistant to fragmentation. Protection of DNA by histone was dependent on nucleosome assembly and did not simply reflect presence of scavenging protein. In contrast to this specific cleavage of internucleosomal linker DNA by iron-ADP, iron-EDTA cleaved polynucleosomes indiscriminately at all sites. The hydroxyl radical scavenger thiourea completely inhibited the random cleavage of polynucleosomes by iron-EDTA but inhibited the nonrandom cleavage of polynucleosomes by iron-ADP less completely, suggesting the possibility that the lower affinity iron-ADP chelate may allow association of free iron with DNA. Thus, oxygen radicals generated by iron-ADP indiscriminately cleaved naked DNA but cleaved chromatin preferentially at internucleosomal bare linker sites, perhaps because of nonrandom iron binding by DNA. These findings suggest that the DNA-damaging effects of iron may be nonrandom, site-directed and modified by histone protein.**

## INTRODUCTION

Cellular metabolism generates reactive oxygen species including superoxide anion and hydrogen peroxide (H<sub>2</sub>O<sub>2</sub>). Trace metals such as iron can catalyze the formation of hydroxyl radical ( $\cdot$ OH) from H<sub>2</sub>O<sub>2</sub>, potentially causing DNA damage (1–3). Oxidative

DNA damage is believed to contribute to the development of cell damage induced by radiation (4,5) and certain chemotherapeutic agents (6,7) and to the development of neoplasia via mutagenic or clastogenic effects (1,5,8). Previous *in vitro* models have examined iron and oxygen radical induced damage to naked DNA unassociated with its histone protein and/or have utilized iron associated with nonphysiologic chelators (6,7,9–11). DNA in its native state in the nucleus, however, is complexed with histone protein in repeating nucleosome units, comprising 140 base pairs (bp) of DNA wound around a central histone octamer (12). The histone octamer together with histone H1 stabilizes 160 bp of DNA and confers resistance to micrococcal nuclease digestion, with unprotected linker DNA, unassociated with protein and of variable length, joining adjacent nucleosome units (13). The relationship between higher order chromatin structure and susceptibility to iron induced oxygen radical damage to DNA is unknown.

In this study, we investigated the possibility that nucleosomal structure might protect the histone-associated DNA from oxidative damage. For these studies we used an oxygen radical damaging system consisting of H<sub>2</sub>O<sub>2</sub>, ascorbate and iron associated with a possible physiologic chelator, ADP (14,15). To investigate the mechanism of interaction of this low-affinity iron chelate with polynucleosomal DNA, we compared its effects with a high affinity iron chelate, iron-EDTA, which generates  $\cdot$ OH in fluid phase and is believed not to bind to DNA (16,17).

## MATERIALS AND METHODS

### Materials

Micrococcal nuclease was obtained from Worthington Biochemical Corp. (Freehold, NJ), the 123 bp ladder and *Hind* III lambda phage DNA molecular weight markers from Bethesda Research Laboratories (Gaithersburg, MD), RNase A from Boehringer Mannheim Biochemicals (Indianapolis, IN), the ion exchange resin AG1-X8 from Biorad Laboratories (Richmond, CA), and deferoxamine mesylate from Ceiba Geigy (Basle, Switzerland). All other reagents, including calf thymus DNA, were purchased from Sigma Chemical Company (St. Louis, MO). Calf thymus DNA was stored over Chelex resin (sodium

\* To whom correspondence should be addressed

form), and nucleosomes and DNA derived from nucleosomes were either stored over resin or dialysed against buffers containing resin just prior to use.

### Polynucleosome and DNA preparation from chicken erythrocyte chromatin

Chromatin was prepared from freshly collected chicken erythrocytes as previously described (18). Washed nuclei were lysed by 1% (v/v) Triton X-100, and the resulting chromatin preparation was digested with micrococcal nuclease (50 units/mg DNA). Following termination of digestion by 5mM Tris-HCl containing 5mM EDTA (pH 7.5), nuclear debris was pelleted by centrifugation, and supernatant polynucleosomes were fractionated by exponential sucrose gradient fractionation. Fractions showed the characteristic absorbance profile at 260 nm of nucleosomes fractionated in this way (not shown). The size of polynucleosome fractions was characterized by gel electrophoresis (see below) and visualized by ethidium bromide staining (Fig. 1). Protein-free control DNA was prepared from polynucleosomes isolated from chicken erythrocyte chromatin by two phenol extractions followed by two chloroform extractions and ethanol precipitation.

### Nucleosome assembly

Nucleosomes were reassembled from calf thymus DNA and chicken erythrocyte core histones as previously described (19). The core histones were prepared from freshly collected chicken erythrocytes. Nuclei were extensively washed and partially digested with micrococcal nuclease (19, 20). After removal of histone H1 by stirring over the ion-exchange resin AG1-X8 (21), histones were salt-extracted by dialysis into 2M NaCl, 5mM Tris-HCl, 0.5mM EDTA, 0.1mM phenylmethylsulfonylfluoride (pH 7.3). Nuclear debris was pelleted by ultracentrifugation (20), and the protein content of the supernatant histone measured by Biorad protein assay was 1mg/ml.

High molecular weight calf thymus DNA was exposed to RNase A (100 $\mu$ g/ml; 37°C for 60 minutes) to remove contaminating RNA, deproteinized by phenol/chloroform extraction, and sheared (30,000 rpm for 30 minutes; Virtis 45 homogenizer) prior to mixing with core histones. Nucleosomes were assembled by mixing DNA and salt-extracted core histones at a histone:DNA ratio of 0.8:1 (22) in 2M NaCl, 0.01% 2-mercaptoethanol, 0.2mM PMSF, 5mM Tris-HCl (pH 7.2). Reconstruction included 8 stepwise 90 minute dialyses against NaCl varying from 2M to 0.05M (19). Nucleosome assembly was verified by micrococcal nuclease digestion (0.2u/ $\mu$ g DNA; 30 minutes) which resulted in digestion to 140 bp DNA fragments when nucleosome assembly was successful.

These nucleosome extraction and reassembly procedures were carried out at 4°C. All buffers and reagents, including those used in subsequent experiments, contained 0.1–0.2 mM phenylmethylsulfonylfluoride to inhibit endogenous nuclease activity, and all were rendered iron-free using Chelex resin, the resin being removed by centrifugation or filtration immediately prior to use.

### Exposure to iron and oxygen radicals

Protein-free DNA (calf thymus or chicken erythrocyte), extracted polynucleosomes, and reassembled nucleosomes were exposed to an oxygen radical generating system comprised of iron (1–500 $\mu$ M), H<sub>2</sub>O<sub>2</sub> (1–500 $\mu$ M) and ascorbate (150–500 $\mu$ M). Iron (FeCl<sub>2</sub>) was used either in the form of a Fe<sup>2+</sup>/ADP chelate (molar ratio 1:2) or of a Fe<sup>2+</sup>/EDTA chelate (molar ratio also

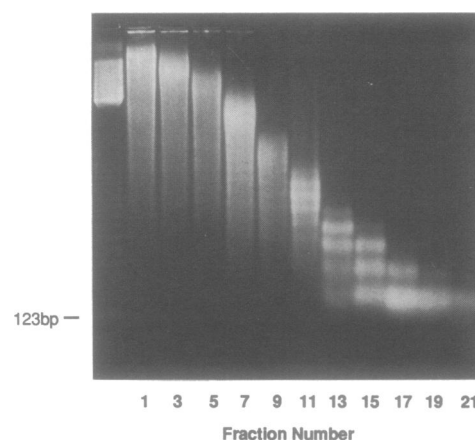


**Figure 1.** Preparation of soluble polynucleosomes. Soluble polynucleosomes from a partial micrococcal nuclease digest of chicken erythrocyte nuclei were fractionated by an exponential sucrose gradient, and DNA extracted from such fractions was electrophoresed in a 0.8% w/v agarose gel. The size marker was a *Hind* III digest of lambda phage DNA. Polynucleosome oligomers represented by fractions 1–3 (or DNA extracted from these fractions) were pooled for use in subsequent experiments.

1:2). The order of reagent addition was: Fe<sup>2+</sup>/ADP (or Fe<sup>2+</sup>/EDTA), DNA or polynucleosomes, buffer, H<sub>2</sub>O<sub>2</sub> and ascorbate (23). The Fe<sup>2+</sup>/ADP, Fe<sup>2+</sup>/EDTA, ascorbate and H<sub>2</sub>O<sub>2</sub> solutions were freshly prepared just prior to use. DNA was 10 $\mu$ g per exposure in experiments using calf thymus DNA and 60 $\mu$ g per exposure in those using polynucleosomes and control chicken erythrocyte DNA. Exposure of polynucleosomes prepared from chromatin and DNA extracted therefrom was in 5mM phosphate, 80mM NaCl (pH 7.2), and exposure of reassembled polynucleosomes and DNA extracted therefrom was in 5mM phosphate, 50mM NaCl (pH 7.2). Exposure was at 37°C for 1 hour, timed from the addition of ascorbate to termination of the reaction with deferoxamine (5mM). In time-response experiments, we found that development of double-strand breaks in DNA began within 20 seconds of oxygen radical exposure, most damage occurred between 5 and 10 minutes, and that damage was maximal at 60 minutes (data not shown).

### Detection of double-strand DNA breaks

Polynucleosomes and monomer nucleosomes were deproteinized by phenol-chloroform and isoamyl alcohol extraction followed by ethanol precipitation. DNA was resuspended in Tris-EDTA and electrophoresed on agarose gels (40mV for 12 hours) following the addition of ethidium bromide directly to samples. DNA was visualized by ultraviolet light and double-strand breaks detected by the appearance of low molecular weight DNA fragments. Data shown are representative of repeated experiments. The extraction process alone did not cause damage to DNA in the form of double-strand breaks (not shown).

## RESULTS

### Fragmentation of protein-free DNA by iron and oxygen radicals

In the presence of ascorbate and H<sub>2</sub>O<sub>2</sub>, iron-ADP extensively damaged DNA causing double-strand breaks at concentrations as low as 1  $\mu$ M iron (Fig. 2A). Iron-mediated degradation of

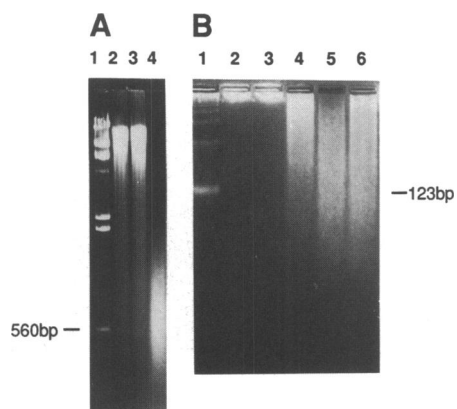


**Figure 2.** Degradation of protein-free DNA by iron-ADP. Double strand breaks were visualized on a 0.8% agarose gel (Panel A). A *Hind* III DNA molecular weight marker is shown in lane 1. Control protein-free calf thymus DNA is shown in lane 2 and DNA exposed only to ascorbate (150 $\mu$ M) and H<sub>2</sub>O<sub>2</sub> (150 $\mu$ M) in the absence of iron in lane 3. DNA exposed to ascorbate (150 $\mu$ M), H<sub>2</sub>O<sub>2</sub> (150 $\mu$ M) and iron (1 $\mu$ M) is shown in lane 4. In panel B, electrophoresis on a 3% Nusieve/1% Seakem agarose gel shows that fragmentation of calf thymus DNA by oxidant damage is random and indiscriminate. Lane 1 shows a 123 bp DNA molecular weight marker. Lane 2 shows control DNA. Lanes 3–6 show DNA exposed to H<sub>2</sub>O<sub>2</sub> (500 $\mu$ M) and ascorbate (500 $\mu$ M); lane 3 was in the absence of iron while lanes 4–6 were in the presence of iron (50, 250, and 500 $\mu$ M, respectively).

protein-free DNA was characterized by random fragmentation covering a wide size range, the smallest fragments being much smaller than the 123 bp DNA molecular weight marker (Fig 2B). Ascorbate and H<sub>2</sub>O<sub>2</sub> alone, in the absence of iron, did not cause appreciable damage to protein-free calf thymus DNA. In dose-response experiments, at 1 $\mu$ M iron-ADP and 500 $\mu$ M ascorbate, DNA double strand breaks increased with increasing H<sub>2</sub>O<sub>2</sub> concentration from 100 to 500 $\mu$ M (data not shown).

#### Exposure of polynucleosomes to iron and oxygen radicals

In contrast to the random fragmentation observed for protein-free DNA, concentrations of iron-ADP up to 250 $\mu$ M iron, with ascorbate and H<sub>2</sub>O<sub>2</sub> converted pooled large molecular weight polynucleosomes (greater than 600 bp, represented by fractions 1–3 in Fig. 1) to monomer and dimer nucleosome forms (Fig. 3A). The size of the monomer band was approximately 160 bp, consistent with the formation of monomer nucleosome particles. At extremely high concentrations of iron (350–500 $\mu$ M), nucleosomal histone protein was no longer able to protect its associated DNA, and random fragmentation with formation of smaller fragments of DNA was evident (Lane 2, Fig 3A). No discernable damage to polynucleosomes was caused by H<sub>2</sub>O<sub>2</sub> and ascorbate in the absence of iron (Fig. 3A).

In contrast to the nucleosomal ladder-like cleavage of polynucleosomes by iron-ADP, protein-free DNA extracted from these polynucleosomes was indiscriminately cleaved when exposed to iron/ascorbate/H<sub>2</sub>O<sub>2</sub> under the same conditions (Fig. 3B). Extensive damage to DNA was evident even at 50 $\mu$ M concentrations of iron-ADP (the lowest concentration used in these experiments) and double-strand breaks were random, with no periodicity of attack or nucleosomal pattern evident. The additional extraction process itself did not alter the susceptibility of DNA to oxidant damage (data not shown).

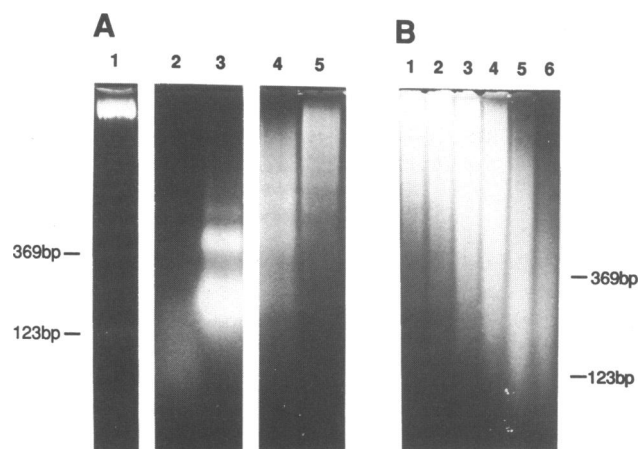


**Figure 3.** Exposure of polynucleosomes to oxidant damage. Chromatin polynucleosome aliquots were exposed to iron/H<sub>2</sub>O<sub>2</sub>/ascorbate, and DNA extracted from each aliquot was electrophoresed on 1.5% Nusieve/0.5% Seakem agarose gel (Panel A). Lane 1 shows the 123 bp DNA molecular weight marker. Lanes 2–5 show DNA from polynucleosomes that were exposed to iron (350, 250 and 50 $\mu$ M and 0 $\mu$ M respectively) in the presence of H<sub>2</sub>O<sub>2</sub> (500 $\mu$ M) and ascorbate (500 $\mu$ M). The control experiment in Panel B shows extensive fragmentation of DNA that was exposed to oxygen radical stress after extraction from the polynucleosomes. Lane 1 shows control protein-free DNA; lanes 2–6 show DNA exposed to H<sub>2</sub>O<sub>2</sub> (500 $\mu$ M) and ascorbate (500 $\mu$ M) and iron (0, 50, 100, 250 and 500 $\mu$ M respectively).

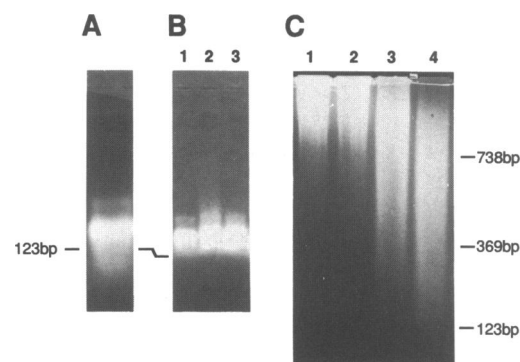


**Figure 4.** Exposure of reassembled nucleosomes to oxidant damage. Panel 4A shows DNA from control reconstituted nucleosomes following partial micrococcal nuclease digestion (1.5% Nusieve/0.5% Seakem agarose gel). Panel 4B shows DNA from these nucleosomes exposed to ascorbate (500 $\mu$ M), H<sub>2</sub>O<sub>2</sub> (500 $\mu$ M) and 100 $\mu$ M (lane 1), 250 $\mu$ M (lane 2) and 500 $\mu$ M (lane 3) iron. Panel 4C shows the protein-free DNA used for the nucleosome assembly experiment. Lane 1 shows control DNA, lanes 2–4 show DNA exposed to ascorbate (500 $\mu$ M) and H<sub>2</sub>O<sub>2</sub> (500 $\mu$ M) in the absence of iron (lane 2), and in the presence of 100 and 250 $\mu$ M iron (lanes 3 and 4 respectively).

#### Exposure of reassembled nucleosomes to iron and oxygen radicals

We also reconstituted nucleosomes from protein-free calf thymus DNA and chicken erythrocyte core histones and exposed them to iron-ADP, H<sub>2</sub>O<sub>2</sub> and ascorbate. The reconstituted nucleosome cores do not contain histone H1 and are associated with approximately 140 bp of DNA (Fig. 4A). These reconstituted nucleosomes were resistant to degradation by iron-ADP even at 500 $\mu$ M concentrations so that nucleosome structure was

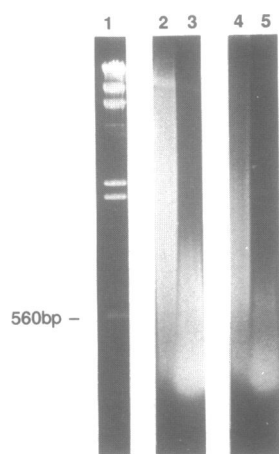


**Figure 5.** Addition of core histones to DNA fails to protect DNA in the absence of nucleosome assembly. Lane 1 shows the *Hind* III DNA molecular weight marker. Lanes 2 and 3 show protein-free DNA exposed to  $H_2O_2$  ( $500\mu M$ ) and ascorbate ( $500\mu M$ ) in the absence and presence of  $100\mu M$  iron, respectively. Core histones were then mixed in a 0.8:1 ratio with calf thymus DNA, and the mixture exposed to  $H_2O_2$  ( $500\mu M$ ) and ascorbate ( $500\mu M$ ) without and with  $100\mu M$  iron (lanes 4 and 5, respectively).

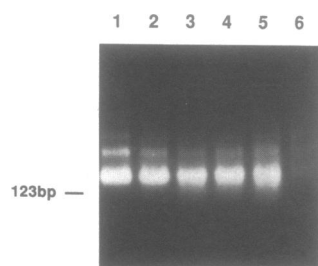


**Figure 6.** Random cleavage of polynucleosomes by iron-EDTA. Polynucleosomes were exposed to increasing concentrations of iron-EDTA/ $H_2O_2$ /ascorbate. DNA was extracted and electrophoresed on a 1.5% Nusieve/0.5% Seakem agarose gel. Lane 1 shows DNA from polynucleosomes that were exposed only to  $H_2O_2$  ( $500\mu M$ ) and ascorbate ( $500\mu M$ ) in the absence of iron. Lanes 2–6 show increasing random fragmentation of polynucleosomes exposed to  $H_2O_2$ , ascorbate and increasing concentrations of iron-EDTA (0.1, 1, 2, 10 and  $50\mu M$  respectively).

conserved (Fig. 4B). In contrast, the protein-free DNA that was used for these nucleosome reassembly experiments was extensively fragmented at  $100\mu M$  iron-ADP (Fig. 4C). This damage to DNA unassociated with histone protein was random, with no evidence of formation of a nucleosome-like pattern and no evidence of a 140 bp particle resistant to fragmentation.

#### Unassembled histone protein fails to protect

Core histone protein mixed directly with calf thymus DNA under conditions not conducive to nucleosome assembly (which we verified by failure to assemble nuclease-resistant nucleosome particles; data not shown) failed to protect DNA against iron-mediated oxygen radical damage (Fig. 5).

#### Random damage to polynucleosomes by iron-EDTA

Cleavage of polynucleosomes by the iron-ADP chelate was compared with damage induced by iron-EDTA, which is known to generate  $\cdot OH$  in fluid phase. By virtue of its electronegativity

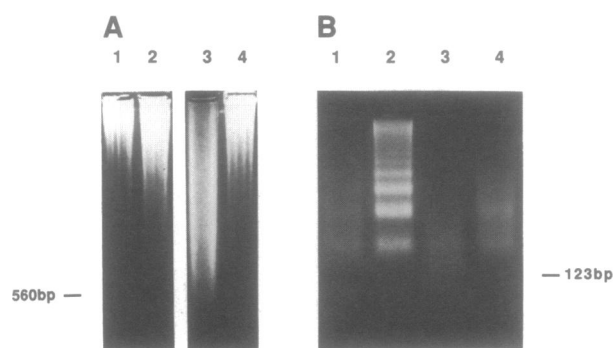


**Figure 7.** Inhibition of iron-mediated damage by thiourea. Panel A shows protection of protein-free calf thymus DNA against iron-ADP mediated oxidant damage. Lane 1 shows control calf thymus DNA. Lane 2 shows DNA exposed only to  $H_2O_2$  ( $500\mu M$ ) and ascorbate ( $500\mu M$ ). Lanes 3 and 4 show DNA exposed to  $50\mu M$  iron-ADP,  $H_2O_2$  and ascorbate in the absence (lane 3) and presence (lane 4) of  $10mM$  thiourea. Thiourea also inhibited DNA damage due to iron-EDTA (not shown). Panel B shows DNA from polynucleosomes that were exposed to  $50\mu M$  iron-EDTA,  $H_2O_2$  and ascorbate (Lanes 1 and 2) and to  $500\mu M$  iron-ADP,  $H_2O_2$  and ascorbate. Thiourea ( $10mM$ ) was present during oxidant exposure in lanes 2 and 4.

this iron chelate is unlikely to bind directly to DNA, and, by virtue of its high affinity for iron, it is unlikely to allow binding of free iron by DNA (16,17). In contrast to the internucleosomal cleavage of polynucleosomes by iron-ADP, iron-EDTA under the same experimental conditions cleaved polynucleosomes indiscriminately, as evidenced by lack of accumulation of a monomer band (Fig. 6). Although iron-EDTA is a more efficient generator of  $\cdot OH$  than is iron-ADP in this experimental system (data not shown), we observed this completely random damage by iron-EDTA even at the lowest iron-EDTA concentrations causing any detectable damage.

#### Influence of thiourea on iron-mediated damage to DNA and polynucleosomes

The addition of the  $\cdot OH$  scavenger thiourea ( $10mM$ ) completely inhibited fragmentation of protein-free calf thymus DNA by low concentrations of iron-ADP (Fig. 7A) and by iron-EDTA (not shown). Random damage to polynucleosomes caused by  $50\mu M$  iron-EDTA was also completely inhibited in the presence of thiourea (Fig. 7B). In contrast, at concentrations of iron-ADP which result in a similar degree of polynucleosome fragmentation, thiourea failed to afford such complete protection (Figure 7, Panel B). This incomplete inhibition by thiourea of iron-ADP mediated polynucleosome cleavage was also seen at lower concentrations of iron-ADP (not shown).

#### DISCUSSION

Oxidant stress potentially exerts clastogenic and mutagenic effects on cells (24–26), can promote transformation (27), and may have some direct carcinogenic capability (28). At the molecular level, oxygen radicals induce a myriad of structural defects in DNA (9,29,30), most likely mediated via hydroxyl radical formation involving a Fenton type mechanism targeted by intranuclear iron (3). It is hypothesized, but not proven, that such damage is mediated by DNA-bound iron (31). Such bound iron complexes could be formed with DNA nucleotides or the phosphate groups of the DNA backbone (3,32). Previous *in vitro* studies of oxidant-

induced damage to cell-free DNA have used unphysiologic iron chelators such as EDTA or methidiumpropyl-EDTA (10,11). Iron-EDTA generates fluid-phase  $\cdot\text{OH}$ , and, by virtue of its electronegativity, this chelate is assumed to be unable to complex with the DNA polyanion (16, 17). In our studies we have used iron in the presence of a possible physiologic chelator, iron/ADP, because ferrous iron/nucleotide complexes catalyse the production of  $\cdot\text{OH}$  radicals from  $\text{H}_2\text{O}_2$  (14, 15), and ADP may be available in cell nuclei.

The observed differences in DNA damage mediated by iron-ADP and iron-EDTA in our study suggest different mechanisms of damage for the two chelates. While naked DNA was extensively and randomly fragmented by as little as  $1\mu\text{M}$  iron-ADP under experimental conditions in which only 1 iron molecule is available per 555 bp of DNA, iron-ADP converted polynucleosomes to monomer nucleosomes. Iron-targeted oxidation preferentially destroyed internucleosomal sites, *i.e.*, DNA unassociated with histone protein. Iron-EDTA-mediated oxidation, however, did not appear to be targeted preferentially to internucleosomal sites, since random cleavage of polynucleosomes with no mononucleosome formation was observed at all iron-EDTA concentrations. Thus, histone protein appears to protect DNA from damage mediated by iron-ADP, but not by iron-EDTA.

The actual mechanisms through which nucleosomal histone protein protects associated DNA from iron-ADP oxidant damage are not proven. It is unlikely that this protection is due to non-specific scavenging of  $\cdot\text{OH}$  or to removal of iron by histone metal binding domains (33), since histone proteins do not protect without nucleosome assembly. Nonrandom internucleosomal  $\cdot\text{OH}$  induced DNA damage cannot be due to sequence specificity, since the same DNA when removed from histone becomes susceptible to random damage. The conformation of DNA in nucleosomes may result in its relative insensitivity to damage, which could result either from decreased inherent susceptibility to  $\cdot\text{OH}$  attack or from altered iron binding by DNA. Our observations argue against a decreased inherent susceptibility, since nucleosomal structure did not protect DNA from damage by fluid phase  $\cdot\text{OH}$  generated by iron-EDTA. We also do not believe that our results can be simply explained by bulk phase shielding conferred by nucleosomal protein, diminishing accessibility of DNA to the damaging agent. There are few contact points between histone protein and DNA in the nucleosome, and DNA residues associated with the core particle still remain accessible to small molecules (34). Moreover, when DNA is attached to a calcium phosphate surface, which should provide an absolute shielding from  $\cdot\text{OH}$  generated in bulk phase, cleavage is modulated (depending upon base proximity to the shielding surface) but still occurs at all base pairs (35).

Our findings using iron-ADP appear to be in contrast to 'hydroxyl radical footprinting' in which the presence of DNA binding proteins is proven by their protection of underlying sequences from iron-EDTA-generated  $\cdot\text{OH}$ -mediated damage (16, 36). However, these nonstructural proteins are generally believed to be bound to DNA in major or minor grooves (36,37) in a manner distinctly different from the association of core histone with DNA wound around the outside of the nucleosomes. A similar iron-EDTA system has been used to corroborate the conformational alteration (periodicity of helical turns) of DNA associated with nucleosomes (38). Indeed, the latter investigation documents that the hydroxyl radical footprinting method using iron-EDTA cleaves DNA at all sites even within the nucleosomal

segment supporting our conclusion that our findings cannot be explained by bulk phase shielding of nucleosomal DNA by histone protein. Thus, prior investigations have not addressed the protective effect of nucleosomal histone protein that we have demonstrated; nor have they investigated the cleavage patterns of alternative iron chelates.

The specific internucleosomal DNA attack by iron-ADP (but not by iron bound to the higher affinity chelator EDTA) suggests that iron-ADP may allow generation of  $\cdot\text{OH}$  at the target site rather than in fluid phase. Evidence that this difference indeed results from differences in site of  $\cdot\text{OH}$  production is suggested by scavenging studies. Although thiourea completely inhibited iron-EDTA cleavage of polynucleosomes, it only incompletely inhibited damage resulting from iron-ADP. Thus, oxidant generated in fluid phase by iron-EDTA is more accessible to scavenging than that generated by iron-ADP, supporting the hypothesis that iron binds directly to DNA when presented as a chelate with ADP (39). It is conceivable that iron-ADP binds as a complex to DNA, but it is more likely that the low affinity chelate liberates free iron which then becomes associated with the target DNA. Indeed, at the concentrations used in these studies, at a 2:1 ADP:iron ratio, and assuming an association constant for the iron:ADP complex of  $10^4$  (40), there would be some free iron not bound to ADP. Consistent with an effect of free iron (or iron-ADP) bound directly to DNA, separate experiments (data not shown) revealed a diminution in DNA damage in proportion to elevation of NaCl concentration.

The pathophysiological significance of our observations remains conjectural since extensive double-strand fragmentation of DNA is required for detection of damage in our system, dictating the use of rather high iron concentrations. Single-strand breaks may be more pathophysiological relevant in terms of the mutagenic effects of iron. However, it is likely that accumulation of double-strand breaks reflects prior development of single-strand breaks in our experimental system. Irradiation models of DNA damage have demonstrated a complex relationship between double- and single-strand breaks by identifying a linear dose-response relationship between  $\cdot\text{OH}$  generation and single-strand breaks and a linear-quadratic dose-response relationship for double-strand breaks (9, 41). We cannot state for certain whether development of double-strand breaks in our system derives entirely from direct conversion of single- to double-strand breaks or whether it derives by accumulation of multiple independent single-strand breaks or whether both processes are involved. In either case, however, the iron-ADP system leads to nonrandom targeting of the oxidant damage to DNA. Since iron-ADP at concentrations less than  $250\mu\text{M}$  nonrandomly cleaved linker areas, it is probable that DNA damage resulting from the low physiologic or pathologic intracellular iron concentrations would also be targeted to these areas. Although nothing is known about the availability of iron in the nucleus in close proximity to DNA, we believe it likely that iron concentrations capable of significant DNA damage can occur, especially in iron overload states.

Thus, our data suggest that histone proteins, which are highly conserved during evolution, may provide a protective role for nuclear DNA *in vivo*. Certain areas of the genome, those not associated with histone protein, may be relatively unprotected against mutagenic damage, and actively transcribing genes, with more 'open' chromatin structure and decreased histone binding to DNA (42), may become preferred targets for oxidant damage. Pathologic conditions characterized by iron-overload such as

hemochromatosis predispose to the development of neoplasia, possibly mediated by the mutagenic effects of iron-targeted oxygen radicals (1,5). In this setting, chromatin structure may provide a protective cellular mechanism against widespread mutagenic effects of iron and oxygen radicals. It is possible, however, that this protective effect inadvertently directs iron-oxidative damage to active genes, especially in actively dividing cells; such damage may result in deregulation of genes involved in cell growth. It seems possible that such mechanisms could contribute to non-random genetic alterations associated with malignant transformation.

## ACKNOWLEDGEMENTS

Supported by the National Institutes of Health (HL30160) and an American Society of Hematology Scholar Award to H.U.E.

## REFERENCES

- Halliwell, B., and Gutteridge, J.M.C. (1984) *Biochem. J.*, **219**, 1–14.
- Imlay, J.A., Chin, S.M., and Linn, S. (1988) *Science*, **240**, 640–642.
- Imlay J.A., and Linn, S. (1988) *Science*, **240**, 1302–1309.
- Ames, B.N. (1983) *Science*, **221**, 1256–1264.
- Halliwell, B. (1987) *FASEB J*, **1**, 358.
- Burger, R.M., Peisach, J., and Horwitz, S.B. (1981) *J. Biol. Chem.*, **258**, 1559–1564.
- Beraldo, H., Garnier-Suillerot, A., Tosi, L., and Lavelle, F. (1985) *Biochemistry*, **24**, 284–289.
- Cerruti, P.A. (1985) *Science*, **227**, 375–381.
- Siddiqui, M.A., and Bothe, E. (1987) *Radiat. Res.*, **112**, 449–46.
- Cartwright, I.L., Hertzberg, R.P., Dervan, P.B., and Elgin, S.C.R. (1983) *Proc. Natl. Acad. Sci. USA*, **80**, 3213–3217.
- Hertzberg, R.P., and Dervan, P.B. (1984) *Biochemistry*, **23**: 3934–3
- Kornberg R.D. (1977) *Ann. Rev. Biochem.*, **46**, 931–954.
- Todd, D and Garrard, W.T. (1977) *J. Biol. Chem.*, **252**, 4729–4738.
- Floyd, J.A. (1983) *Arch. Biochem. Biophys.*, **225**, 263–270.
- Gutteridge, J.M.C., Zs-Nagy, I, Maidt, L and Floyd, R.A. (1990) *Arch. Biochem. Biophys.*, **227**, 422–428.
- Tullius, T.D., Dombroski, B.A., Churchill, M.E.A., and Kam, L. (1987) *Meth. Enz.*, **155**, 537–559.
- Celander, D.W., and Cech T.R. (1990) *Biochemistry*, **29**, 1356–1361.
- Allan, J., Nicolas, R.H., and Goodwin, G.H. (1986) in MacGillivray, A.J., and Birnie, G.D. (eds.) *Nuclear Structures: Isolation and Characterization*, Butterworths, Stoneham, pp. 47–73.
- Jorcano, J.L., and Ruiz-Carrillo, A. (1979) *Biochemistry*, **18**, 768–774.
- Ruiz-Carrillo, A., and Jorcano, J.L. (1979) *Biochemistry*, **18**, 760–767.
- Thoma, F., Koller, T., and Klug, A. (1979) *J. Cell Biol.*, **83**, 403–427.
- Ruiz-Carrillo, A., Jorcano, J.L., Eder, G., and Lurz, R. (1979) *Proc. Natl. Acad. Sci. USA*, **76**, 3284–3288.
- Cohen, G. (1985) in Greenwald, R.A. (ed.), *Handbook of Methods for Oxygen Radical Research*. CRC Press, Boca Raton, Florida, pp. 55–64.
- Schraufstatter, I., Hyslop, P.A., Jackson, J.H., and Cochrane, C.G. (1988) *J. Clin. Invest.*, **82**, 1040–1050.
- Weitzman, S.A., and Stossel, T.P. (1981) *Science*, **212**, 546–547.
- Weitzberg, A.B., Weitzman, S.A., Destremes, M., Latt, S.A., and Stossel, T.P. (1983) *NEJM*, **308**, 26–29.
- Zimmerman, R., and Cerutti, P. (1984) *Proc. Natl. Acad. Sci. USA*, **81**, 2085–2087.
- Weitzman, S.A., Weitzberg, A.B., Clark, E.P., and Stossel, T.P. (1985) *Science*, **227**, 1231–1233.
- Hutchinson, F. (1985) *Prog. Nuc. Acid. Res. and Molec. Biol.*, **32**, 115–154.
- Denq, R-Y., and Fridovich, I. (1989) *Free Rad. Biol. Med.*, **6**, 123–129.
- Samuni, A., Aronovitch, J., Godinger, D., Chevion, M., and Czapski, G. (1983) *Eur. J. Biochem.*, **137**, 119–124.
- Sissoeff, I., Grisvard J., and Guille, E. (1976) *Prog. Biophys. Molec. Biol.*, **31**, 165–199.
- Berg, J.M. (1986). *Science*, **232**, 485–487.
- van Holde, K.E. (1989) *Chromatin*, Springer-Verlag, New York, 219–288.
- Tullius, T.D., and Dombroski, B.A. (1985) *Science*, **230**, 679–681.
- Tullius, T.D., and Dombroski, B.A. (1986) *Proc. Natl. Acad. Sci. USA*, **83**, 5469–5473.
- Dervan P.B. (1986) *Science*, **232**, 464–471.
- Hayes, J.J., Tullius, T.D., and Wolffe A.P. (1990) *Proc. Natl. Acad. Sci. USA*, **87**, 7405–7409.
- Halliwell, B., and Gutteridge, J.M.C. (1990) *Meth. Enz.*, **186**, 1–85.
- Tu, A.T., and Heller, M.J. (1974) in Sigel H (ed.) *Metal ions in Biological Systems*, Marcel Dekker, inc., New York, 19–31.
- Bohne, L., Coquerelle, T., and Hagen, U. (1970) *Int. J. Radiat. Biol.*, **17**, 105–215.
- Nacheva, G.A., Guschin, D.Y., Preobrazhenskaya, O.V., and Karpov V.L. (1989) *Cell*, **58**, 27–36.